

## **Effect of boron on the microstructure of hydrogenated microcrystalline silicon thin films**

**A. Dussan<sup>1</sup> and R. R. Koropecski<sup>2</sup>**

<sup>1</sup> Dpto. Física, Universidad Nacional de Colombia, Bogotá

<sup>2</sup> INTEC (CONICET -UNL), Güemes 3450, 3000 Santa Fe, Argentina

Received 16 October 2006, revised 23 November 2006, accepted 30 May 2007

Published online 26 October 2007

**PACS** 61.10.Nz, 68.37.Ps, 68.55.-a, 73.61.Cw, 78.30.Am, 81.15.Gh

In this work, a series of boron doped microcrystalline silicon films ( $\mu\text{c-Si:H}$  (B)) were deposited by plasma-enhanced chemical vapor deposition (PECVD), using silane ( $\text{SiH}_4$ ) diluted in hydrogen, and diborane ( $\text{B}_2\text{H}_6$ ) as a dopant gas. The concentration of  $\text{B}_2\text{H}_6$  was varied in the range of 0–100 ppm. The microstructure and morphology of samples were analyzed by atomic force microscopy (AFM), X-ray diffraction (XRD), and Raman spectroscopy. A trend towards increasing crystalline volume fraction and grain size were observed as boron concentration in the samples increased; while the XRD spectra show that the peak intensity at  $2\theta \approx 47^\circ$  decreases and becomes gradually amorphous with the increasing degree of doping. The doped microcrystalline silicon films presented a crystallographic preferential orientation in the plane (220). Correlations between structural and electric properties were also studied.

phys. stat. sol. (c) **4**, No. 11, 4134–4138 (2007) / DOI 10.1002/pssc.200675915

## Effect of boron on the microstructure of hydrogenated microcrystalline silicon thin films

A. Dussan<sup>\*1</sup> and R. R. Koropecski<sup>\*\*2</sup>

<sup>1</sup> Dpto. Física, Universidad Nacional de Colombia, Bogotá

<sup>2</sup> INTEC (CONICET -UNL), Güemes 3450, 3000 Santa Fe, Argentina

Received 16 October 2006, revised 23 November 2006, accepted 30 May 2007

Published online 26 October 2007

PACS 61.10.Nz, 68.37.Ps, 68.55.-a, 73.61.Cw, 78.30.Am, 81.15.Gh

In this work, a series of boron doped microcrystalline silicon films ( $\mu\text{-Si:H}$  (B)) were deposited by plasma-enhanced chemical vapor deposition (PECVD), using silane ( $\text{SiH}_4$ ) diluted in hydrogen, and diborane ( $\text{B}_2\text{H}_6$ ) as a dopant gas. The concentration of  $\text{B}_2\text{H}_6$  was varied in the range of 0–100 ppm. The microstructure and morphology of samples were analyzed by atomic force microscopy (AFM), X-ray diffraction (XRD), and Raman spectroscopy. A trend towards increasing crystalline volume fraction and grain size were observed as boron concentration in the samples increased; while the XRD spectra show that the peak intensity at  $2\theta \approx 47^\circ$  decreases and becomes gradually amorphous with the increasing degree of doping. The doped microcrystalline silicon films presented a crystallographic preferential orientation in the plane (220). Correlations between structural and electric properties were also studied.

© 2007 WILEY-VCH Verlag GmbH & Co. KGaA, Weinheim

### 1 Introduction

Hydrogenated microcrystalline silicon films have received great attention during the last few years, due to their potential applications in optoelectronic devices such as thin film transistors [1], solar cells [2, 3] and many other applications. The incorporation of boron in  $\mu\text{-Si:H}$  films has produced excellent window-contact-layer material for photovoltaic devices due to better optoelectronic properties in comparison with the p-type hydrogenated amorphous silicon (a-Si:H) [4]. The study and understanding of the optical, structural and electric properties have been the object of numerous investigations but all of them are based on deposition parameters [5, 6]; such as the hydrogen–silane dilution ratio ( $R = [\text{H}_2]/[\text{SiH}_4]$ ); the effect produced by the degree of boron compensation in this material, on its micro structure, and the correlation among the other properties had not been established till now.

In this paper we present the results of structural characterization of doped boron  $\mu\text{-Si:H}$  films, obtained by means of atomic force microscopy (AFM), X-ray diffraction (XRD) and Raman spectroscopy measurements. The films were compensated, by varying  $\text{B}_2\text{H}_6$  gas concentration from 0 to 100 ppm. We found that preferential growth orientation of (220) and grain size of silicon crystallites are influenced by the degree of boron compensation. Finally, we found a correlation between micro doping and electric properties.

\* Corresponding author: e-mail: adussanc@unal.edu.co

\*\* e-mail: rkoro@intec.ceride.gov.ar

## 2 Experimental details

The  $\mu\text{-Si:H(B)}$  samples were prepared in a capacitive coupled HF-PECVD reactor working at a frequency of 50 MHz. A description of the characteristics and the operational conditions of the reactor were reported elsewhere [7]. Corning 7059 glass was used as substrate and the deposition temperature was 150 °C. The reaction gas was a mixture of 94% hydrogen and 6% silane, containing diborane in the range of 0–100 ppm. Total flux and pressure were kept constant at 20 sccm and  $4.5 \times 10^{-1}$  Torr, respectively.

The Raman spectra of the  $\mu\text{-Si:H(B)}$  were measured with a Micro-Raman in the Ecole Polytechnique Laboratory of France. 20 mW laser power was used for these measurements, with a 10X objective and 3 minute time exposure. All Raman spectra were measured at room temperature. The crystalline volume fraction  $X_C$  was estimated from the Raman spectra by deconvoluting the spectra into crystalline ( $520 \text{ cm}^{-1}$ ), and amorphous ( $480 \text{ cm}^{-1}$ ) peaks, and a third peak around  $510 \text{ cm}^{-1}$ , associated with the dilatation of the Si-Si bonds in the grain boundaries [8], which is also influenced by mechanical stress in the films [9]. The study of the morphological properties was carried out with a Park Scientific AFM microscope. Microcrystallinity of the samples was confirmed by X-ray diffraction (XRD) studies. The X-ray diffraction spectra were collected by means of a Phillips diffractometer. (goniometer PW 1820)

Conductivity measurements were carried out in a cryostat using thermally evaporated aluminium interdigitated electrodes. They were 25 cm in length and separated 0.01 cm from each other. The electrical current was measured with a Keithley 617 electrometer connected to a computer. The samples were annealed at 420 K and then cooled down to 120 K at a constant rate of 1.5 K/min. The applied field was 1000 V/cm.

## 3 Results and discussion

Starting from the deconvolution of the Raman spectra, the crystalline volume fraction ( $X_C$ ) was obtained, using the relation reported in previous studies [10]. The values corresponding to  $X_C$  obtained for the  $\mu\text{-Si:H}$  samples are reported on Table 1. We also notice that the increase in boron concentration induces a change in the amorphous-crystalline transition, showing an increase in  $X_C$  for samples with 0 to 75 ppm concentrations; whereas a decrease in this parameter may be observed when the boron concentration is 100 ppm (see Table 1). This fact is related to an amorphization in the material when there are greater doping concentrations [10].

**Table 1** Structural parameters and electric conductivity of the boron doped microcrystalline silicon samples.  $X_C$ : crystalline volume fraction;  $Z$ : grain size from AFM images; RMS - roughness;  $\sigma_{dk}$ : dark conductivity –  $T = 300 \text{ K}$ ;  $E_a$ : activation energy.

Ratio $[\text{B}_2\text{H}_6]/[\text{SiH}_4]$ (ppm)	$X_C$ (%)	$Z$ (Å)	RMS (Å)	$\sigma_{dk}$ (cm. $\Omega$ ) <sup>-1</sup>	$E_a$ (eV)
0	33.47	513	59.8	$1.40 \times 10^{-4}$	0.29
12.5	54.77	562	90	$1.30 \times 10^{-5}$	0.36
25	55.82	564	92.1	$2.43 \times 10^{-8}$	0.68
50	61.21	986	105	$3.01 \times 10^{-6}$	0.37
75	60.88	1040	84.7	$1.35 \times 10^{-6}$	0.38
100	52.38	1510	93.6	$1.28 \times 10^{-5}$	0.33

Figure 1a shows the XRD spectra obtained for the  $\mu\text{-Si:H(B)}$  samples. The XRD spectrum of the c-Si appears as reference at the bottom of the graph. A clear microcrystalline structure may be observed in all the samples, with a preferential orientation in the plane (220). The diffracted peak that is shown for  $2\theta \approx 25^\circ$  degrees, may be attributed to Si-O bonds forming  $\text{SiO}_2$  [11].

The peak associated with the plane of growth for the group of  $\mu\text{c-Si:H(B)}$  samples ( $2\theta \approx 47^\circ$  degrees), is shown in detail in Fig. 1b. In this figure we notice a systematic increase in the intensity-width relation of the diffraction peak as the boron concentration increases from 0 to 75 ppm; whereas, for a concentration of 100 ppm, its intensity decreases drastically. The above agrees with the Raman measures, where, for major boron concentrations ( $> 75$  ppm),  $X_C$  decreases in the samples, clearly showing an amorphous characteristic in the material.

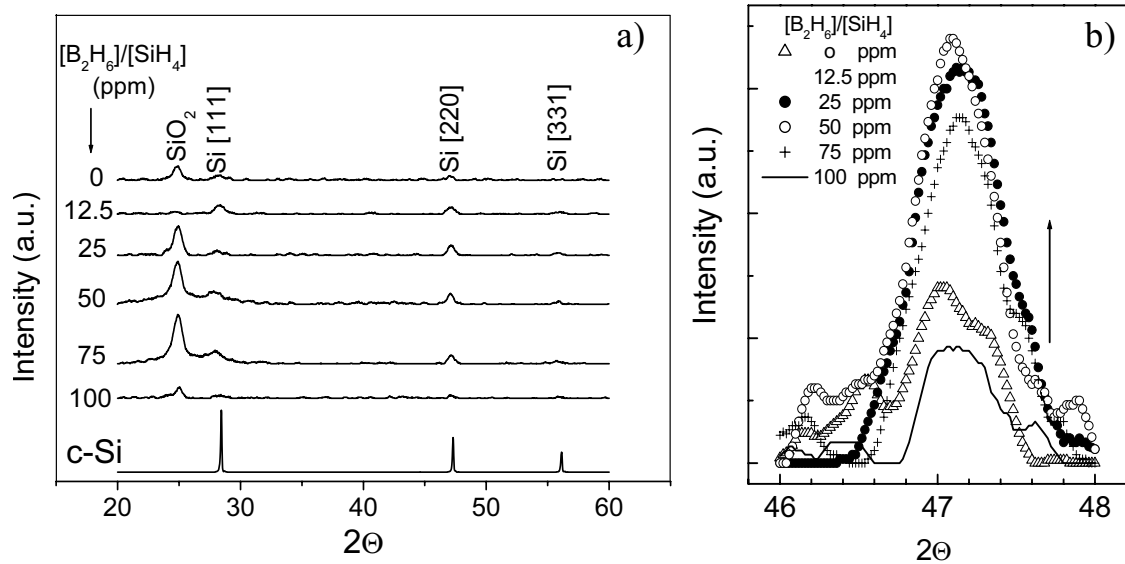


**Fig. 1** a) XRD spectra of different boron-doped  $\mu\text{c-Si:H}$  films. The spectra are arbitrarily shifted vertically for the sake of clarity. b) Detail of (220) peak diffracted of each boron doped  $\mu\text{c-Si:H}$  sample.

AFM measurements produced information regarding the morphological properties of the  $\mu\text{c-Si:H}$  thin films doped with boron. Figure 2 shows AFM images of  $\mu\text{c-Si:H}$  samples.

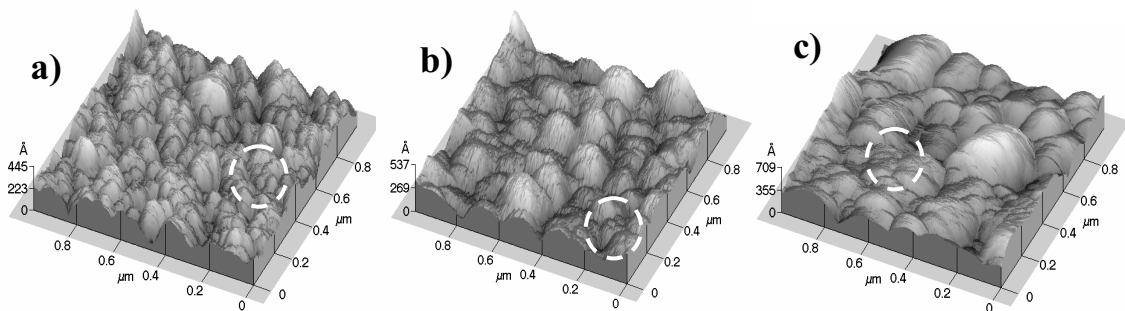
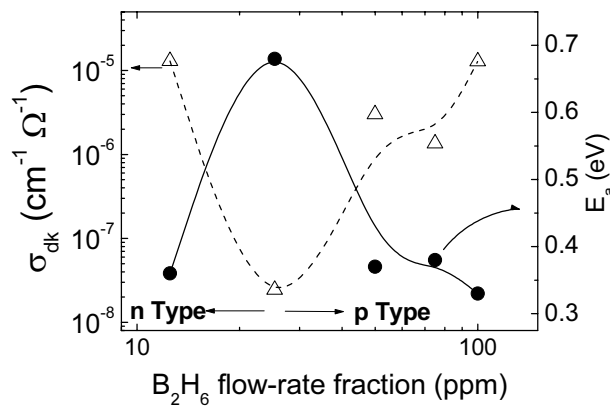


**Fig. 2** AFM images of microcrystalline silicon hydrogenated with different boron concentration. a) 0 ppm, b) 75 ppm and d) 100 ppm. A circle around each image indicates the presence of smaller crystal substructures.

Figure 2 shows an increase in grain size in the  $\mu\text{c-Si:H}$  samples as boron concentration increases in the material. On the other hand, we can see that the roughness in the samples is not greatly affected by the incorporation of boron concentrations above 0 ppm. The values corresponding to average grain size and roughness (RMS), from AFM measurements, are shown on Table 1. The grain size value was also obtained from the diffraction spectra, using the Debye-Scherrer equation [12]. In this last case, the crystal

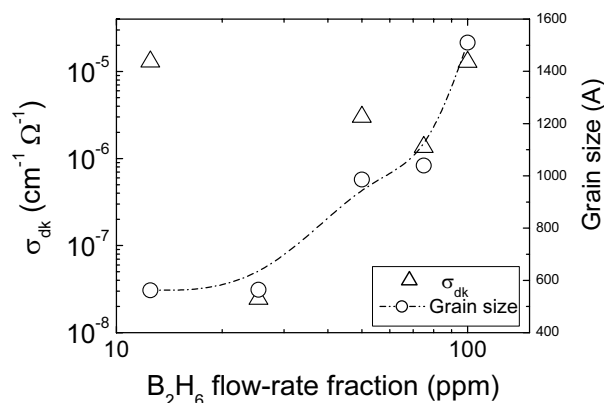
size values obtained ( $\sim 10 \text{ \AA}$ ) differ significantly from those obtained through AFM images (see Table 1). This can be explained by the presence of regions of much smaller crystals growing between grains that stand out on the surface (see the regions marked with circles in Fig. 2). The presence of these substructures in the samples was detected when those regions were magnified and thus the average grain size was obtained. The values found are in accordance with the one obtained through the XRD spectra.

Figure 3 shows room temperature dark conductivity  $\sigma_{\text{dk}}$ , and the activation energy  $E_a$ , for each one of the  $\mu\text{-Si:H}$  samples with different concentrations of  $\text{B}_2\text{H}_6$  in the state in which they were deposited.  $E_a$  was obtained from the slope in the Arrhenius graph of the dark conductivity curves according to inverse temperature, for the high temperature region where the behavior of these curves is linear.



**Fig. 3** Room temperature dark conductivity and activation energy for  $\mu\text{-Si:H}$  samples with different boron doping degrees. The lines are drawn to guide the eye.

The variation in activation energy caused by boron incorporation in the samples indicates a change in the behavior of the semiconductor from that of a type  $n$  material, for the sample deposited with 0 ppm of boron, to a type  $p$  material, when boron concentration reaches 100 ppm (see Fig. 3). A compensated state is obtained when the boron concentration is 25 ppm. Thermopotency measurements at room temperature allowed a verification of the type  $n$  or  $p$  characteristics of the material. Small quantities of boron, which act as impurity acceptors produce large variations in the  $\sigma_{\text{dk}}$ , as may be seen in Fig. 3.



**Fig. 4** Room temperature dark conductivity and grain size average for  $\mu\text{-Si:H}$  samples with different boron doping degrees. The line is drawn to guide the eye.

The electrical and transport properties for  $\mu\text{c-Si:H}$  samples micro-doped with boron have been studied previously [13]. An increase in the  $\sigma_{\text{dk}}$  value for samples with concentrations above 25 ppm was observed (see Fig. 4).

## 4 Conclusions

In this paper we have presented a study of the effect of boron micro-doping on the structure of hydrogenated microcrystalline silicon thin films using various concentrations of diborane. We found that the increase of boron in the material produces an increase in the size of the crystals, but no significant change in surface roughness was observed. We detected the existence of a substructure dominated by regions of much smaller crystals growing between grains that stand out on the surface. A progressive increase in the crystalline volume fraction for concentrations from 0 to 75 ppm was detected; whereas, in a boron concentration of 100 ppm, we observed a reduction of crystalline fraction, which indicates an amorphization of the material. It was established, using electric conductivity measurements, that a variation in boron concentration induces a change of behavior in the material from type n (for concentrations below 25 ppm) to type p (for concentrations above 25 ppm). A correlation between the structural and electric properties of this material was found.

**Acknowledgements** This work was partially supported with ANPCyT grants (PICT 12-06950). We thank the Semiconductors and Solar Cells group for the XRD measurements.

## References

- [1] Y. Chen and S. Wagner, *Appl. Phys. Lett.* **75**, 1125 (1999).
- [2] A. Shah, J. Meier, E. Vallat-Sauvain, N. Wyrsh, U. Kroll, C. Droz, and U. Graf, *Sol. Cells* **78**, 469 (2003).
- [3] O. Vetterl, F. Finger, R. Carius, P. Hapke, L. Houben, O. Kluth, A. Lambert, A. Muck, B. Rech, and H. Wagner, *Sol. Cells* **62**, 97 (2000).
- [4] J. Meier, S. Dubail, R. Fluckiger, H. Keppner, and A. Shah, *Appl. Phys. Lett.* **65**, 860 (1994).
- [5] M. Goerlitzer, P. Torres, N. Beck, N. Wyrsh, H. Keppner, J. Pohl, and A. Shah, *J. Non-Crys. Solids* **227–230**, 996 (1998).
- [6] H. Chen and W. Z. Shen, *Surf. Coat. Technol.* **198**, 98 (2005).
- [7] S. B. Concari, R. H. Buitrago, M. T. Gutierrez, and J. J. Gandia, *J. Appl. Phys.* **94**, 2417 (2003).
- [8] C. Das and S. Ray, *Thin Solid Films* **403/404**, 81 (2002).
- [9] Ch. Ossadnik, S. Veprek, and I. Gregora, *Thin Solid Films* **337**, 148 (1999).
- [10] R. Saleh and N. H. Nickel, *Thin Solid Films* **427**, 266 (2003).
- [11] Liwei Li, Yuan-Min Li, J. A. Anna Selvan, A. E. Delahoy, and R. A. Levy, *J. Non-Cryst. Solids* **347**, 106 (2004).
- [12] B. D. Cullity, *Elements of X-ray Diffraction* (Addison Wesley, Reading, MA, 1978), p. 283.
- [13] A. Dussan and R. H. Buitrago, *J. Appl. Phys.* **97**, 043711 (2005).